DOI: 10.1002/glia.24516

# RESEARCH ARTICLE



# Pyruvate dehydrogenase kinase 2 knockdown restores the ability of amyotrophic lateral sclerosis-linked SOD1G93A rat astrocytes to support motor neuron survival by increasing mitochondrial respiration

Adriana Cassina Patricia Cassina De la Patricia Cassina Dela Patricia Cassina De la Patricia De la Patricia

#### Correspondence

Patricia Cassina, Departamento de Histología y Embriología, Facultad de Medicina, Universidad de la República, Av. Gral, Flores 2125, 11800 Montevideo, Uruguay. Email: pcassina@fmed.edu.uy; patricia.cassina@gmail.com

# **Funding information**

Programa de Desarrollo de las Ciencias Básicas (PEDECIBA); Agencia Nacional de Investigación e Innovación, Grant/Award Number: FCE\_1\_2019\_1\_156461

# **Abstract**

Amyotrophic lateral sclerosis (ALS) is characterized by progressive motor neuron (MN) degeneration. Various studies using cellular and animal models of ALS indicate that there is a complex interplay between MN and neighboring non-neuronal cells, such as astrocytes, resulting in noncell autonomous neurodegeneration. Astrocytes in ALS exhibit a lower ability to support MN survival than nondiseaseassociated ones, which is strongly correlated with low-mitochondrial respiratory activity. Indeed, pharmacological inhibition of pyruvate dehydrogenase kinase (PDK) led to an increase in the mitochondrial oxidative phosphorylation pathway as the primary source of cell energy in SOD1G93A astrocytes and restored the survival of MN. Among the four PDK isoforms, PDK2 is ubiquitously expressed in astrocytes and presents low expression levels in neurons. Herein, we hypothesize whether selective knockdown of PDK2 in astrocytes may increase mitochondrial activity and, in turn, reduce SOD1G93A-associated toxicity. To assess this, cultured neonatal SOD1G93A rat astrocytes were incubated with specific PDK2 siRNA. This treatment resulted in a reduction of the enzyme expression with a concomitant decrease in the phosphorylation rate of the pyruvate dehydrogenase complex. In addition, PDK2-silenced SOD1G93A astrocytes exhibited restored mitochondrial bioenergetics parameters, adopting a more complex mitochondrial network. This treatment also decreased lipid droplet content in SOD1G93A astrocytes, suggesting a switch in energetic metabolism. Significantly, PDK2 knockdown increased the ability of SOD1G93A astrocytes to support MN survival, further supporting the major role of astrocyte mitochondrial respiratory activity in astrocyte-MN interactions. These results suggest that PDK2 silencing could be a cell-specific therapeutic tool to slow the progression of ALS.

#### KEYWORDS

ALS, astrocytes, mitochondria, PDK2

<sup>&</sup>lt;sup>1</sup>Departamento de Histología y Embriología, Facultad de Medicina, Universidad de la República, Montevideo, Uruguay

<sup>&</sup>lt;sup>2</sup>Departamento de Bioquímica, Centro de Investigaciones Biomédicas (CEINBIO), Facultad de Medicina, Universidad de la República, Montevideo, Uruguay

# 1 | INTRODUCTION

Amyotrophic lateral sclerosis (ALS) is a progressive neurodegenerative disease characterized by the gradual loss of motor neurons (MNs) in the spinal cord, brain stem, and motor cortex, which in turn induce voluntary muscle atrophy (Al-Chalabi et al., 2016). The cellular mechanisms determining neuronal death are still under research, and many have been proposed, including mitochondrial dysfunction (Smith et al., 2019). In ALS patients and animal models of the disease, reactive astrocytes surround both upper and lower degenerating MNs, and evidence indicates that they play a crucial role in the pathology (Taylor et al., 2016). Successive studies have shown that surrounding glial cells, particularly astrocytes, critically influence MN survival (Clement et al., 2003). Co-culture assays have clearly stated a reduced ability of astrocytes to support MN survival in ALS models, whether the cells originate from embryonic stem cells (Di Giorgio et al., 2007), human induced pluripotent stem cells (IPSC) (Haidet-Phillips et al., 2011), mice (Nagai et al., 2007), or rat cells (Vargas et al., 2006). We have previously described that a metabolic switch characterized by reduced mitochondrial respiration underlies the astrocyte-mediated toxicity to MNs (Miguel et al., 2012). In primary astrocyte cultures obtained from the transgenic (Tg) ALS-linked mutated SOD1G93A rats (SOD1G93A astrocytes), treatment with the metabolic modulator dichloroacetate (DCA) enhanced both their mitochondrial respiratory activity and ability to support MN survival in co-culture. In addition, DCA administration to SOD1G93A mice reduced neuronal death and increased survival (Miguel et al., 2012). DCA is an inhibitor of the pyruvate dehydrogenase kinases (PDKs), which phosphorylate the  $E1\alpha$  subunit of the pyruvate dehydrogenase (PDH) complex (PDC) and suppress the catalysis of pyruvate to acetyl-CoA (Holness et al., 2003). Inhibition of PDK keeps most of PDH in the active form, and therefore, pyruvate metabolism switches towards glucose oxidation to CO2 in the mitochondria. The PDH/PDK system acts as a key regulator of mitochondrial respiration. It plays an essential role in the metabolic switch from oxidative phosphorylation (OXPHOS) to aerobic glycolysis that accompanies malignant transformation in cancer (Zhang et al., 2015).

PDC is a multisubunit protein that is composed of PDH (E1), dihydrolipoyl acetyltransferase (E2), dihydrolipoyl dehydrogenase (E3), and E3-binding protein (E3BP) subunits that concertedly convert pyruvate to acetyl-CoA (Patel & Roche, 1990). All subunits are expressed in astrocytes and neurons, but astrocytes show significantly higher immunoreactivities for all of them than neurons (Halim et al., 2010).

Besides the differential expression of its constituent proteins, PDC activity is regulated by several mechanisms, such as allosteric inhibition by acetyl CoA and NADH. However, the main mechanism for maintaining long-term control over metabolic processes is through covalent modification of the enzyme. The reversible phosphorylation of PDH- $E1\alpha$  that regulates PDC activity (Patel & Korotchkina, 2006) is accomplished by four different PDKs (PDK1-4) and two different phosphatases (PDP1-2), which are all differentially expressed in mammalian tissues (Bowker-Kinley et al., 1998). The regulation of PDC at the

protein expression or activity levels contributes to the differential metabolic phenotype of neurons and astrocytes (Halim et al., 2010). In addition, there are different expression levels of PDH kinases and phosphatases between both cell types (Halim et al., 2010). Indeed, control of PDK expression levels allows cells and tissues to regulate PDC activity and, therefore, glucose oxidation rates and mitochondrial respiration (Lydell et al., 2002). While PDK1 and PDK3 are present in both cell types, with slightly higher expression of PDK1 in neurons, PDK2 and PDK4 levels are significantly superior in astrocytes compared with neurons (Halim et al., 2010), which is consistent with the higher PDH $\alpha$ phosphorylation status, lower PDC activity, and higher lactate production displayed by these cells (Pellerin & Magistretti, 2012). These different profiles of PDK isoform expression between astrocytes and neurons offer a key target to regulate mitochondrial respiration specifically in astrocytes. In particular, the PDK2 isoform has been previously reported to be enhanced in astrocytes during diabetes, where it determines phosphorylated-PDH (p-PDH), causing a glycolytic metabolic shift along with substantial inflammation (Rahman et al., 2020,) which prompted us to select this isoform for this study.

Here, we tested the hypothesis of whether silencing PDK2 may enhance mitochondrial respiratory function in SOD1G93A expressing astrocytes and, in turn, improve their capacity to support MN survival.

#### 2 | MATERIALS AND METHODS

# 2.1 | Materials

Culture media and serum were from Gibco (Thermo Fisher Scientific). Culture flasks and plates were from Nunc (Thermo Fisher Scientific). siRNAs were purchased from Ambion (Thermo Fisher Scientific). DCA and all other reagents were from Sigma-Aldrich (Merck) unless otherwise specified.

#### 2.2 | Ethics statement

Procedures using laboratory animals were in accordance with international guidelines and were approved by the Institutional Animal Committee: Comisión Honoraria de Experimentación Animal de la Universidad de la República (CHEA; https://chea.edu.uy/); protocol # 1038.

#### 2.3 | Animals

Rats (*Rattus norvegicus*) were housed (up to six female or male animals per cage) in a centralized animal facility with a 12-h light–dark cycle with ad libitum access to food and water. Male hemizygous NTac:SD-Tg (SOD1G93A) L26H rats (RRID:IMSR\_TAC:2148), obtained from Taconic (Hudson, NY), were bred locally with outbred Sprague–Dawley background. The progenies were genotyped by polymerase chain reaction (PCR), as previously described (Howland et al., 2002).

# 2.4 | Primary cell cultures

Neonatal rat astrocyte cultures were prepared from Tg SOD1G93A or non-Tg 1-day-old pups (without regard to sex) genotyped by PCR, according to the procedures of Saneto and De Vellis (1987) with minor modifications (Cassina et al., 2002). Briefly, spinal cords were dissected, meninges were carefully removed, and tissue was chopped and dissociated with 0.25% trypsin-EDTA for 25 min at 37°C. Trypsinization was stopped with high glucose (4.5 g/L), pyruvate-free Dulbecco's modified Eagle's medium (DMEM) supplemented with 4-(2-hydroxyethyl)piperazine-1-ethane-sulfonic acid (HEPES, 3.6 g/L), penicillin (100 IU/mL), streptomycin (100 mg/mL), and 10% (v/v) fetal bovine serum (FBS) (s-DMEM medium) in the presence of 50 µg/mL DNase I. After mechanical disaggregation by repeated pipetting, the suspension was passed through an 80-µm mesh and spun for 10 min at  $300 \times g$ . The pellet was resuspended in s-DMEM medium and plated at a density of  $1.5 \times 10^6$  cells per 25-cm<sup>2</sup> tissue culture flask. When confluent, cultures were shaken for 48 h at 250 rpm, incubated for another 48 h with 10 μM cytosine arabinoside, and then plated at a density of  $2 \times 10^4$  cells/cm<sup>2</sup> in 4-well plates for co-cultures, Seahorse xFE24 plates for respirometry assays, or Lab-Tek 4-well chambered cover glass for mitochondrial or lipid droplets imaging studies.

Astrocyte-MN co-cultures: MN preparations were obtained from embryonic day 15 (E15) rat spinal cord by a combination of optiprep (1:10, SIGMA St. Louis, MO) gradient centrifugation and immunopanning with the monoclonal antibody IgG192 against p75 neurotrophin receptor as previously described (Cassina et al., 2002), then plated on rat astrocyte monolayers at a density of 300 cells/cm² and maintained for 48 h in Leibovitz's L-15 medium supplemented with 0.63 mg/mL bicarbonate, 5  $\mu$ g/mL insulin, 0.1 mg/mL conalbumin, 0.1 mM putrescine, 30 nM sodium selenite, 20 nM progesterone, 20 mM glucose, 100 IU/mL penicillin, 100  $\mu$ g/mL streptomycin, and 2% horse serum (s-L15 medium) as described (Cassina et al., 2002). Astrocyte treatments were done 24 h prior to MN addition, and the astrocyte monolayers were washed twice with phosphate-buffered saline (PBS) to remove traces of the different treatments before plating the MNs.

# 2.5 | siRNA transfection

A total of 80% confluent spinal cord astrocyte monolayers were changed to DMEM supplemented with 2% FBS before treatment. siRNA transfection was performed using Lipofectamine 2000 (Invitrogen) according to the manufacturer's instructions. Astrocytes were transfected with 40 nM of Silencer Select predesigned siRNAs (Ambion) targeting PDK2 mRNA, PDK1 mRNA, or negative control siRNA (NC siRNA no. 1) 24 h before either total RNA isolation using TRIzol reagent (Invitrogen) for quantitative PCR or 48 h before lysis for western blot or before co-culture experiments. Three different siRNA for PDK2 were tested, and the sequence that achieved a more pronounced reduction of PDK2 expression was selected for the rest of the studies.

#### 2.6 | Western blot

Astrocyte monolayers were treated with siRNA as described above, or 5 mM DCA. After 48 h of treatment, proteins were extracted from cells in 1% sodium dodecyl sulfate (SDS) supplemented with 2 mM sodium orthovanadate and complete protease inhibitor cocktail (Roche). Lysates were resolved by electrophoresis on 12% SDSpolyacrylamide gels and transferred to a nitrocellulose membrane (Thermo). The membrane was blocked for 1 h at room temperature (RT) in 5% bovine serum albumin (BSA) in PBS-T (PBS with 0.1% Tween). The membrane was then probed overnight with primary antibodies in 5% BSA in PBS-T at 4°C, washed in PBS-T, and probed with the appropriate secondary antibodies for 60 min at RT. Primary antibodies were rabbit polyclonal phosphodetect anti-PDH-E1a (pSer293) (AP1062; Calbiochem; RRID:AB\_10616069; 1:800), mouse anti-PDH E1-alpha subunit (Abcam Cat# ab110334, RRID:AB\_10866116; 1:800), and mouse anti-β-actin (Sigma-Aldrich Cat# A5441, RRID:AB 476744; 1:4000) as loading control. The secondary antibodies used were IRDye® 800CW goat anti-mouse IgG antibody (LI-COR Biosciences Cat# 926-32210, RRID:AB 621842) and IRDye® 680RD goat antirabbit IgG antibody (LI-COR Biosciences Cat# 925-68071, RRID:AB 2721181). Detection and quantification were performed with a LI-COR Odyssey imaging system and included software. The relative levels of pSer293 E1a PDH and total E1a PDH were quantified. The pSer293 to total E1a ratio was calculated and normalized against vehicle-treated cells.

#### 2.7 | Quantitative polymerase chain reaction

Total astrocyte RNA was isolated using TRIzol reagent (Thermo Fisher Scientific), followed by chloroform extraction and isopropanol precipitation. Possible DNA contaminations were eliminated with DNase treatment using DNase-free kit (Thermo Fisher Scientific). RNA quality was evaluated by agarose gel electrophoresis followed by ethidium bromide staining and quantified using a NanoDrop 1000 Spectrophotometer (Thermo Fisher Scientific; RRID:SCR 016517). A total of 500 ng of this total RNA was reverse-transcribed using 200 U M-MLV-reverse transcriptase (Thermo Fisher Scientific) following manufacturer instructions. A total of 25 ng of the resulting cDNA was diluted in Biotools Quantimix Easy master mix (Biotools) in 10 µL volume. All reactions were performed in triplicates in strip tubes (Axygen), using specific forward and reverse primers. The sequences of the quantitative polymerase chain reaction (qPCR) primers (IDT, Integrated DNA Technologies) used were as follows: for GAPDH F: 5'-CAC TGA GCA TCT CCC TCA CAA-3' and R: 5'-TGG TAT TCG AGA GAA GGG AGG-3', for PDK2 F: 5'- TCA GCT AGG GGC CTT CTC TT-3' and R: 5'- CCG TAC CCC AGG GGA TAG AT-3'. According to the sample, we used cycles 15-23 (the threshold cycle, Ct) to calculate the relative amounts of our gene of interest. PCR amplification was done over 40 cycles using a Rotor-Gene 6000 System (Corbett Life Science), and data were analyzed using Rotor-Gene 6000 software (Corbett Life Science; RRID:SCR\_017552). Quantification was

performed with the  $\Delta\Delta Ct$  method using astrocytes treated with vehicle as a NC and GAPDH mRNA as reference.

## 2.8 Oxygen consumption rate assays

Oxygen consumption rate (OCR) and extracellular acidification rate (ECAR) were measured simultaneously in a Seahorse XFe24 extracellular flux analyzer (Agilent; RRID:SCR\_019539). Before the experiment, the culture medium was replaced with an unbuffered medium (DMEM pH 7.4, supplemented with 5 mM glucose, 1 mM sodium pyruvate, 32 mM NaCl, and 2 mM glutamine) and incubated for 1 h at 37°C without CO2. Basal oxygen consumption measurements were taken at the beginning of the assay, followed by the sequential addition of oligomycin (0.5 µM), carbonyl cyanide 4-(trifluoromethoxy)phenylhydrazone (FCCP; 2 μM), and antimycin A (AA;  $1 \mu M$ ) + rotenone ( $1 \mu M$ ). The following bioenergetics parameters were determined: basal respiration: (last OCR measurement before oligomycin injection)-(minimum OCR after rotenone/ antimycin A addition); proton leak: (oligomycin-resistant respiration)-(minimum OCR after rotenone/antimycin A addition); respiration linked to ATP production: (last OCR measurement before oligomycin injection)-(minimum OCR after oligomycin addition); maximal respiration: (maximum OCR after FCCP addition)-(minimum OCR after rotenone/antimycin A addition); spare respiratory capacity: maximal respiration—basal respiration. After each assay, protein content (in micrograms) per well was determined with the bicinchoninic acid technique. OCRs and ECARs were normalized considering protein content (in micrograms). Respiratory Indexes were determined as ratios between the respiratory rates obtained in different conditions, which are therefore internally normalized and independent of cell number or protein mass (Brand & Nicholls, 2011). These include coupling efficiency (ratio between respiration linked to ATP synthesis and basal respiration) and respicontrol ratio (RCR; the ratio between maximum and oligomycin-resistant respiration rates).

# 2.9 | Fluorescent labeling of mitochondria

Confluent astrocyte monolayers seeded on 4-well Nunc<sup>TM</sup> LabTek<sup>TM</sup> chambered cover glass (Thermo Scientific) were treated as indicated above with vehicle, NC siRNA, PDK2 siRNA, or 5 mM DCA. After 48 h, the cells were incubated with 100 nM MitoTracker Green FM (Thermo/Invitrogen, Cat# M7514) in DMEM for 30 min in a 37°C incubator at 5% CO<sub>2</sub> and 95% humidity. Following incubation, cells were washed in warm DMEM and visualized by confocal microscopy. Confocal image stacks were acquired with a Leica TCS-SP5-II confocal microscope (Leica Microsystems) using an HCX PL APO 63x/1.40 oil immersion objective, with 0.2  $\mu$ m z-stack slice intervals and at least 10 slices per cell. Images were obtained for at least 25 cells per group from four independent experiments.

# 2.10 | Mitochondrial morphology analysis

Confocal image stacks were deconvolved with Huygens Professional version 19.10 (Scientific Volume Imaging, the Netherlands). Mitochondrial morphology was analyzed using Fiji (ImageJ) software (NIH; RRID:SCR\_002285) as follows: image stacks corresponding to individual cells were extracted from each confocal stack. Images were converted to binary by thresholding and processed to remove noise and outlier voxels. Mitochondrial skeleton profiles were obtained with the built-in skeletonize feature, and morphology was analyzed with the skeleton analysis plugin, which measures the length of each branch and the number of branches in each skeletonized feature, from which parameters describing mitochondrial network morphology were calculated. Distinct mitochondrial morphologies were identified and classified as individuals (puncta and rods) or networks as previously reported (Leonard et al., 2015; Valente et al., 2017): punctate mitochondria are defined as small pointlike structures, whereas rods are elongated without being branched. Networks are characterized by connected branches. In the skeleton analysis. individuals (puncta or rods) have no junctions, while networks are structures with at least one junction. We quantified the number of "individual" structures with no branches (puncta and rods), the number of networks, mean mitochondrial length, and mean length of rods/network branches (mean rod/branch length). For this last parameter, we considered rods and network branches together (puncta are not included), as the biological forces increasing rod length and those increasing the length of network branches should essentially be the same (Valente et al., 2017). Data from at least 25 cells per treatment were analyzed and repeated in four independent experiments.

# 2.11 | Lipid droplets labeling and quantification

Subconfluent astrocyte monolayers seeded on 4-well Nunc™ Lab-Tek™ chamber slides (Thermo Scientific) were treated as indicated above with vehicle, NC siRNA, PDK2 siRNA, or 5 mM DCA in DMEM with 2% foetal bovine serum. Fourty-eight hours later, cells were washed with PBS, fixed with 4% paraformaldehyde in PBS for 18 min on ice, and washed twice with PBS. Then, cells were permeabilized with 0.2% Triton X-100 in PBS for 30 min followed by incubation with blocking solution (BS): 10% goat serum, 2% bovine serum albumin, 0.1% triton X-100 in PBS for 1 h at RT. Cells were incubated overnight with rabbit anti-glial fibrillary acidic protein antibody (1:500; Sigma-Aldrich #G9269, RRID:AB\_477035) in BS at RT, followed by washing three times in PBS and incubation with Alexa Fluor 488-conjugated goat anti-rabbit IgG secondary antibody (1:1000, Thermo Fisher Scientific, # A-11034, RRID:AB\_2576217) for 1 h at RT. After washing twice with PBS, cells were incubated for 30 min at RT with Oil Red O (ORO) working solution (ORO stock solution: 0.625% ORO in 99% [vol/vol] isopropyl alcohol prepared by stirring for 2 h at RT; ORO working solution: 1.5 parts of ORO stock solution to one part of distilled water, incubated for 10 min at 4°C, and filtered through a 45-µm filter to remove precipitates). Following incubation, cells were washed thrice with deionized water, incubated with Hoechst 33342 (1 µg/mL; SigmaAldrich #14533) for 15 min at RT to label nuclei, and mounted in 80% glycerol in PBS. Cell images were acquired using a Nikon Eclipse E400 epifluorescence microscope (Nikon) coupled with a Nikon Ds-Fi3 camera, using a  $40\times$  objective. At least 25 images were obtained per group from three independent experiments. Lipid droplet (LD) quantification: LD images were binarized by thresholding using Fiji (ImageJ) software (NIH; RRID:SCR\_002285), followed by watershed processing to resolve overlapping structures. Particles in each image were counted and analyzed using the "analyze particles" command. The number of LD per cell was estimated as the ratio of LD to the number of nuclei in each image.

#### 2.12 | MN survival assay

Co-cultures were fixed (4% paraformaldehyde plus 0.1% glutaraldehyde in PBS, 15 min on ice) and washed twice with PBS. Then, cells were permeabilized with 0.2% Triton X-100 in PBS for 30 min followed by incubation with BS: 10% goat serum, 2% bovine serum albumin, 0.1% triton X-100 in PBS for 1 h at RT. Cells were incubated overnight with rabbit anti-beta-III tubulin antibody (1:3000; Abcam, #ab18207 RRID: AB\_444319) in BS at 4°C. After washing three times with PBS, cells were incubated with horseradish peroxidase-conjugated goat anti-rabbit IgG secondary antibody (1:500, Thermo Fisher Scientific, #31,460, RRID: AB\_228341) for 1 h at RT, followed by three washes with PBS and 3,3′-diaminobenzidine developing. MN survival was evaluated by direct counting of cells displaying neurites longer than four cell bodies diameter (Cassina et al., 2002; Martínez-Palma et al., 2019) using a Nikon Eclipse TE 200 microscope.

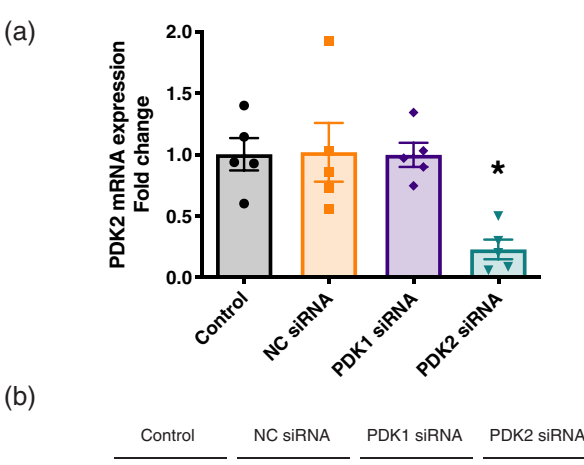
# 2.13 | Statistics

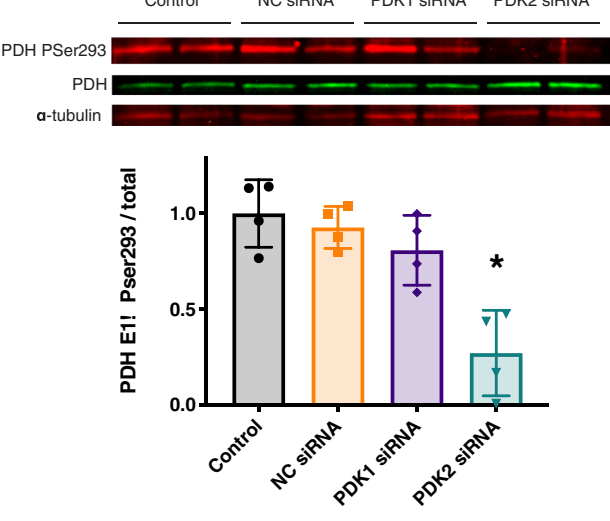
All data analysis and statistics were performed using GraphPad Prism 9 software (RRID:SCR\_002798). Data are presented as mean  $\pm$  SEM of values obtained from at least three independently prepared cultures performed in duplicates or triplicates. Tests used were ordinary one-way ANOVA followed by Tukey's post hoc multiple comparisons. Statistical signification was determined at p < .05.

#### 3 | RESULTS

# 3.1 | Silencing PDK2 mRNA reduced phosphorylated PDH in cultured astrocytes

To downregulate PDK2 expression in cultured astrocytes, confluent astrocyte monolayers were incubated with siRNA for PDK2, PDK1, or NC siRNA without targets, then, PDK2 mRNA expression was detected by qPCR. A reduction in PDK2 mRNA expression was successfully achieved only when siRNA against PDK2 was employed (Figure 1a). Neither PDK1 siRNA nor the NC demonstrated any downregulation of PDK2 mRNA expression.





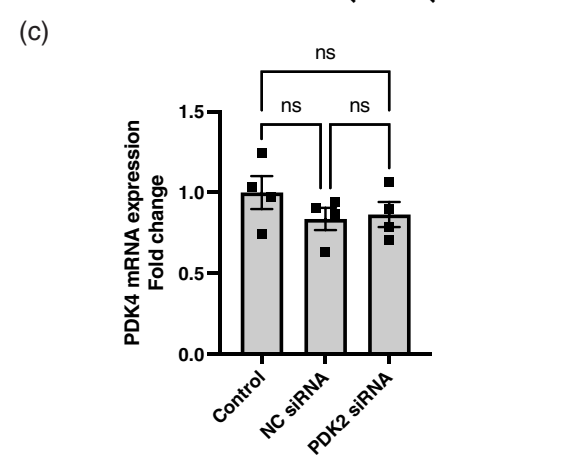


**FIGURE 1** Pyruvate dehydrogenase kinase 2 (PDK2) siRNA treatment reduced PDK2 mRNA expression and PDK activity in astrocytes. (a) PDK2-relative mRNA expression in astrocytes treated with PDK2 siRNA, PDK1 siRNA, negative control siRNA (NC siRNA), and control astrocytes, quantified by qPCR. (b) Relative levels of phosphorylated pyruvate dehydrogenase (PDH) and total PDH in cultured astrocytes. Top pane: representative western blot using antibodies against phosphorylated PDH (PDH PSer293), total PDH E1α, and α-tubulin as loading control of protein samples of astrocytes treated with PDK2 siRNA, PDK1 siRNA, and NC siRNA of vehicle. Bottom pane: phosphorylated PDH/total PDH ratio quantification. (c) PDK4-relative mRNA expression in astrocytes treated with PDK2 siRNA, NC siRNA, or in control astrocytes. All data are presented as mean ± SEM from 4 to 5 independent experiments. \*p < .05; \*\*p < .01; \*\*\*p < .001.

Notably, PDK activity, assessed as the ratio of phosphorylated to total PDH measured by immunoblotting against specific antibodies, was significantly decreased in PDK2 siRNA-treated astrocytes with no variation in total PDH immunoreactivity (Figure 1b). No phosphorylated/total PDH ratio difference was found in PDK1 siRNA or NC siRNA-treated astrocytes.

Furthermore, PDK2 siRNA specifically targeted the PDK2 isoform and did not affect PDK4 mRNA expression, which is the other isoform highly expressed in astrocytes (Guttenplan et al., 2020; Halim et al., 2010; Hasel et al., 2021; Zhang et al., 2014) (Figure 1c).

# 3.2 | PDK2 mRNA knockdown in SOD1G93A expressing astrocytes increases mitochondrial bioenergetic parameters

To study whether PDK2 knockdown could increase the mitochondrial respiration of SOD1G93A astrocytes, confluent SOD1G93A astrocytes were incubated with siRNA for PDK2 or NC siRNA, and OCR was measured before and after the addition of specific inhibitors and an uncoupler of the respiratory chain and OXPHOS as indicated in methods. As previously

reported (Miquel et al., 2012), reduced respiratory capacity was detected in SOD1G93A astrocytes compared with non-Tg astrocytes. Silencing PDK2 mRNA or DCA exposure enhanced OCR in SOD1G93A astrocytes to the extent found in the non-Tg ones (Figure 2a).

SOD1G93A astrocytes exhibited reduced basal, ATP production linked, and maximal respiration compared with non-Tg astrocytes (Figure 2b), as previously reported for other SOD1G93A-expressing cell types (Pharaoh et al., 2019). Upon PDK2 siRNA or DCA treatment, ATP production linked and maximal respiration were significantly increased in SOD1G93A astrocytes (Figure 2b). No significant change in basal respiration was observed following PDK2-siRNA or DCA treatment. No changes were seen in nonmitochondrial or proton leak respiration in any treatment group. In addition, spare respiratory capacity and the respiratory indexes coupling efficiency and RCR were reduced in SOD1G93Aexpressing compared with non-Tg astrocytes (Figure 2c). This indicates a reduced ability of the electron transport chain to respond to an increase in energy demand, a lower coupling of the electron transport chain to ADP phosphorylation, and a diminished overall mitochondrial respiratory function, respectively (Brand & Nicholls, 2011). PDK2 knockdown or DCA treatment showed a significant increase in all these indexes to the level shown by non-Tg astrocytes.

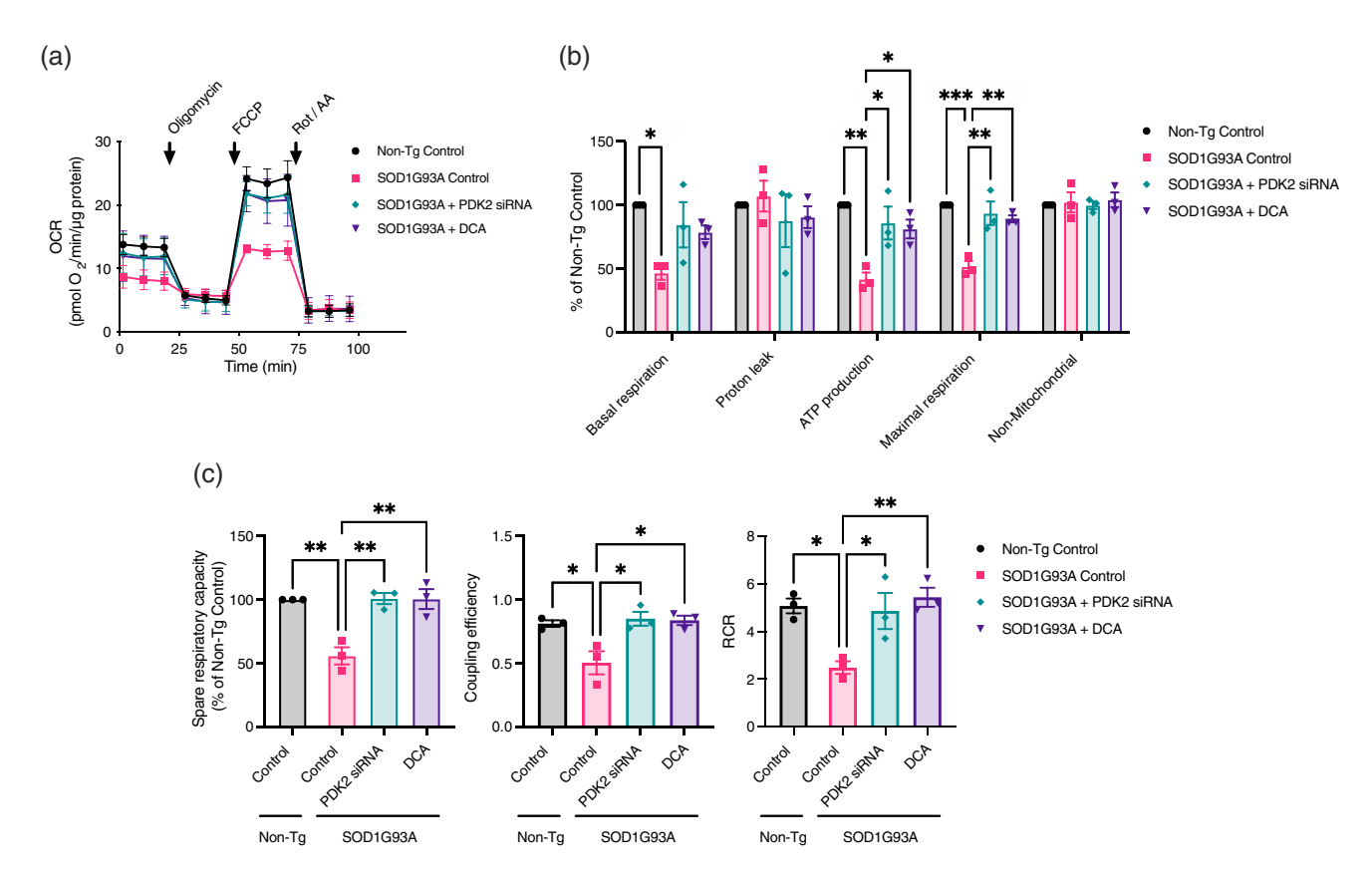


**FIGURE 2** Pyruvate dehydrogenase kinase 2 (PDK2) knockdown improves the mitochondrial function of SOD1G93A-expressing astrocytes. (a) Representative slope curves of the oxygen consumption rate (OCR) for non-Tg and SOD1G93A astrocytes (control and treated with PDK2 siRNA or dichloroacetate [DCA] over time). Arrows indicate the time of addition of oligomycin, carbonyl cyanide 4-(trifluoromethoxy) phenylhydrazone (FCCP), and rotenone + antimycin A (AA). (b) Respiratory parameters (basal respiration, proton leak respiration, respiration linked to ATP production, maximal, and nonmitochondrial respiration) obtained from the OCR profiles of the different treatment groups. Data are expressed as % of non-Tg control. (c) Spare respiratory capacity, coupling efficiency, and cell respiratory control ratio (RCR) of the same treatment groups. All data are presented as mean ± SEM from three independent experiments. \*p < .05; \*\*p < .01; \*\*\*p < .001.

# 3.3 | PDK2 mRNA knockdown in SOD1G93A astrocytes modifies mitochondrial network morphology

The improvement of mitochondrial respiratory function in PDK2-silenced SOD1G93A astrocytes was associated with morphological changes in the mitochondrial network as detected by live confocal microscopy with mitotracker green labeling (Figure 3). After imaging processing involving binarization and skeleton analysis, two types of mitochondrial structures were recognized: networks (mitochondrial structures with at least three branches) and individuals (isolated mitochondria, which could be punctate —a single pixel in the skeletonized image— or rods—unbranched structures with two or more pixels in the skeletonized image—), as previously reported (Bakare et al., 2021; Valente et al., 2017). Smaller

individual mitochondria and more fragmented networks were found in SOD1G93A astrocytes compared with the filamentous mitochondrial network morphology exhibited by non-Tg astrocytes (Figure 3a). This is in agreement with previous reports on SOD1G93A-expressing glial cells (Jiménez-Riani et al., 2017; Joshi et al., 2019; Martínez-Palma et al., 2019). In contrast, when treated with DCA or PDK2 siRNA, SOD1G93A astrocytes exhibit a mitochondrial network morphology reminiscent of that of non-Tg astrocytes (Figure 3a). Consequently, mean mitochondrial length (including all branches), as well as mean mitochondrial rod/branch length (mean length of rod-like mitochondria or branches in mitochondrial networks), was significantly reduced in SOD1G93A astrocytes compared with non-Tg ones (Figure 3b). These parameters were increased in PDK2 siRNA or DCA-treated SOD1G93A astrocytes to the level of non-Tg astrocytes but were not in NC siRNA-

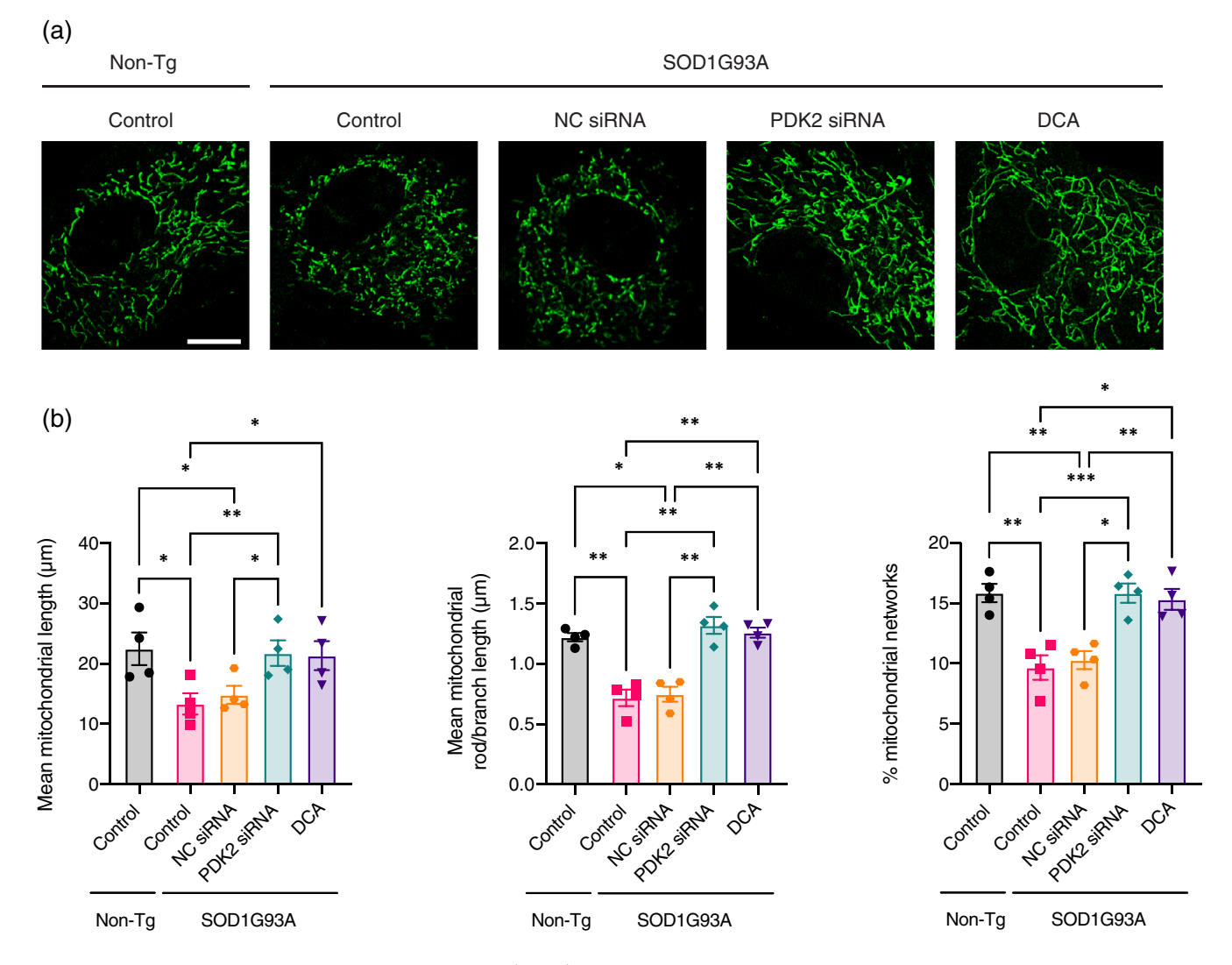


FIGURE 3 Effects of pyruvate dehydrogenase kinase 2 (PDK2) silencing on SOD1G93A-expressing astrocyte mitochondrial network structure. (a) Representative images of mitotracker green-labeled non-Tg or SOD1G93A astrocyte mitochondria in control conditions or treated with negative control siRNA (NC siRNA), PDK2 siRNA, or dichloroacetate (DCA). Scale bar:  $10 \mu m$ . (b) Mitochondrial network morphological parameters: mean mitochondrial length, mean mitochondrial rod/branch length, and percentage of mitochondria forming networks (three or more branches), obtained from the different treatment groups. All data are presented as mean  $\pm$  SEM from four experiments. \*p < .05; \*\*p < .01; \*\*\*p < .001.

treated SOD1G93A astrocytes (Figure 3b). In addition, the percentage of mitochondria adopting a network-like interconnected morphology was reduced in SOD1G93A astrocytes (where there was a higher percentage of isolated mitochondria) compared with non-Tg astrocytes, and it was significantly increased in the case of cells treated with PDK2 siRNA or DCA, to a similar level as in non-Tg astrocytes.

# 3.4 | PDK2 knockdown reduced lipid droplets accumulation in SOD1G93A astrocytes

Inhibition of mitochondrial respiration is associated with lipid droplet accumulation in various cell types, including glial cells (Liu et al., 2015). In addition, SOD1G93A-expressing glial cells exhibit increased lipid inclusions (Jiménez-Riani et al., 2017). Therefore, we analyzed whether PDK silencing may affect these organelles in SOD1G93A astrocytes. Examination of ORO-stained astrocytes showed cytoplasmic accumulation of labeled round bodies of varying size surrounding the cell nucleus, an image consistent with LD (Figure 4a). LD exhibited a heterogeneous distribution across the astrocyte monolayer. Quantification of the number of LDs per cell revealed the previously reported increase in the number of LDs in SOD1G93A astrocytes (Velebit et al., 2020) relative to non-Tg astrocytes. Importantly, there was a significant reduction in LD following

silencing or pharmacological inhibition of PDK2 in SOD1G93A astrocytes (Figure 4b).

# 3.5 | PDK2 knockdown enhanced the ability of SOD1G93A astrocytes to support MN survival

Next, the effect of PDK2 silencing on SOD1G93A astrocyte toxicity to MNs was assessed. As previously reported (Vargas et al., 2006), SOD1G93A astrocytes exhibited a reduced ability to support MN survival compared with non-Tg ones. The number of MNs that survived after 72 h on top of SOD1G93A astrocyte monolayers was reduced by ~50% compared with that obtained from non-Tg astrocyte/MN co-cultures. Silencing PDK2 mRNA on SOD1G93A-expressing astrocytes significantly increased MN survival in co-culture to the level reached on top of non-Tg astrocytes or DCA-treated SOD1G93A astrocytes. In addition, incubation of SOD1G93A with NC siRNA had no effect on MN survival (Figure 5a).

#### 4 | DISCUSSION

Herein, we demonstrate that downregulation of the major astrocytic PDK isoform (PDK2) expression in SOD1G93A-bearing astrocytes

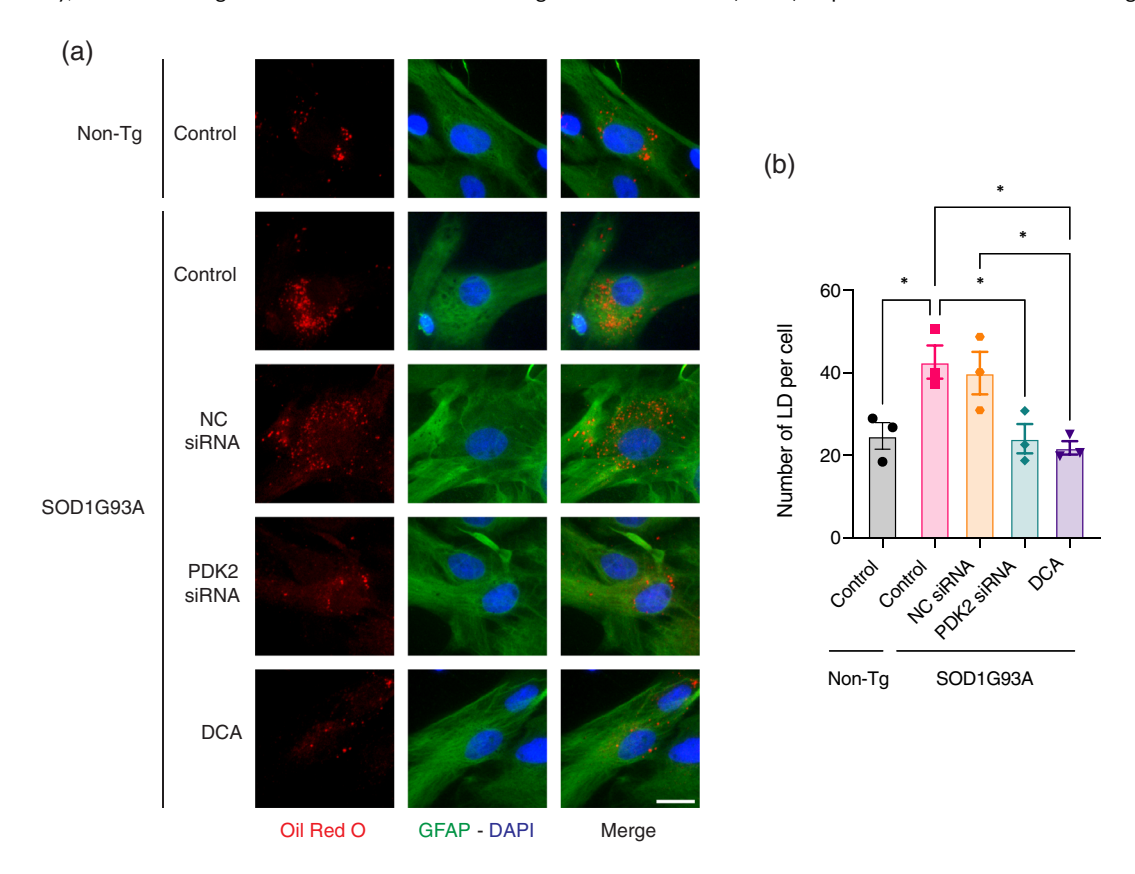
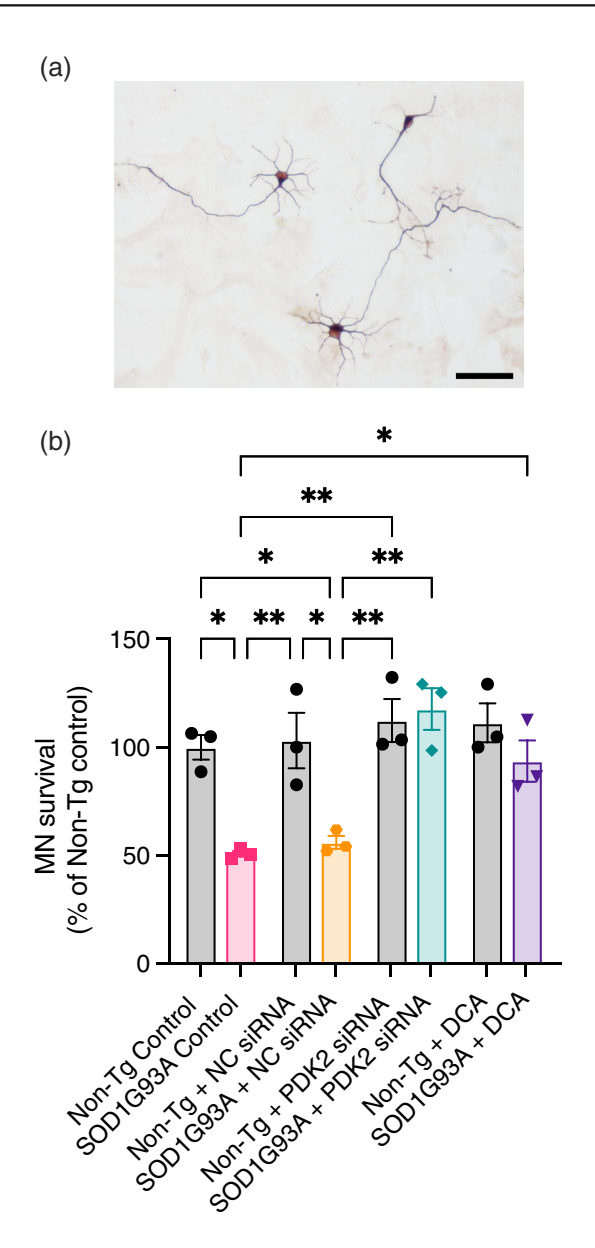


FIGURE 4 Pyruvate dehydrogenase kinase 2 (PDK2) knockdown alters lipid droplet accumulation in SOD1G93A astrocytes.

(a) Representative images from non-Tg or SOD1G93A astrocyte monolayers treated as indicated, stained with Oil Red O to label lipid droplet (LD) (red), and processed for glial fibrillary acidic protein (GFAP) immunofluorescence (green) and Hoechst 33342 for nuclei labeling (blue). Scale bar: 20 µm. (b) Quantification of the mean number of Oil Red O-stained structures per cell in the indicated groups. All data are presented as mean ± SEM from three independent experiments. \*p < .05. DCA, dichloroacetate; NC siRNA, negative control siRNA.



**FIGURE 5** Pyruvate dehydrogenase kinase 2 (PDK2) knockdown recovers the ability of SOD1G93A astrocytes to support motor neuron (MN) survival. (a) Representative image of an astrocyte-motor neuron co-culture processed for βIII-tubulin immunocytochemistry for motor neuron survival quantification. Scale bar: 100 μm. (b) Non-Tg motor neuron survival on top of non-Tg or SOD1G93A astrocyte monolayers following incubation with PDK2 siRNA, negative control (NC) siRNA, or dichloroacetate (DCA). Data are presented as the percentage of MN survival on top of a non-Tg astrocyte monolayer (control). All data are presented as mean ± SEM from three experiments. \*p < .05; \*\*p < .01; \*\*\*p < .001.

modulates the energy phenotype profile, inducing a metabolic switch characterized by an increase in mitochondrial respiratory function and a remodeling of the mitochondrial network morphology to the level of non-Tg astrocytes. Importantly, this selective mRNA knockdown improves the ability of SOD1G93A astrocytes to support MN survival. Our results further strengthen the hypothesis that mitochondrial function in astrocytes is crucial to sustaining MN survival in ALS.

Cell-to-cell communication critically influences MN survival in ALS. We and others have reported that SOD1G93A astrocytes and aberrant glial cells selectively kill surrounding MN (Di Giorgio et al., 2007; Díaz-Amarilla et al., 2011; Nagai et al., 2007; Vargas et al., 2006). We have proposed that a metabolic reprogramming characterized by reduced mitochondrial respiratory activity with a decreased capacity to respond to energetic demands occurs in SOD1G93A expressing astrocytes, which is critically associated with the reduced ability to maintain MN survival (Cassina et al., 2021). This was supported by the results of treating SOD1G93A astrocytes with the metabolic modulator DCA (Miquel et al., 2012). DCA-treated astrocytes presented increased mitochondrial bioenergetics and improved MN survival in co-culture. On top of that, oral administration of DCA to SOD1G93A animals increased survival associated with higher mitochondrial respiratory activity in the spinal cord and delayed MN survival, suggesting that metabolic modulation may offer a new therapeutic target to delay disease progression.

A key target in metabolic modulation is the PDC, a mitochondrial gatekeeping enzyme that links glycolysis with the citric acid cycle and the subsequent OXPHOS (Patel & Roche, 1990; Takubo et al., 2013). PDC is a large complex containing three core enzymatically active subunits: PDH, dihydrolipoamide acetyltransferase, and dihydrolipoyl dehydrogenase (Hiromasa et al., 2004; Hitosugi et al., 2011). PDH directly oxidizes pyruvate (Fan et al., 2014) and harbors regulatory serine residues that act as phosphorylation targets (Kolobova et al., 2001). The PDC is under tight and complex regulation by PDK isoforms 1-4, with expression in peripheral and central tissues (Jha et al., 2012). The previously mentioned role of DCA as a metabolic modulator is based on its known action as a PDK inhibitor, with positive effects on ALS models (Martínez-Palma et al., 2019: Miguel et al., 2012; Palamiuc et al., 2015). A more recently described PDK inhibitor, phenylbutyrate, has also shown promising effects in ALS (Del Signore et al., 2009; Paganoni et al., 2020; Ryu et al., 2005), even exhibiting a synergistic effect with DCA (Ferriero et al., 2015). The PDK2 isoform is one of the most abundant in astrocytes (Halim et al., 2010) and exhibits negligible expression levels in neurons. PDK2 isoform knockdown resulted in reduced PDK2 expression in cultured astrocytes and, more importantly, diminished PDH phosphorylation, leading to increased OXPHOS activity. Indeed, bioenergetic mitochondrial parameters and indexes were significantly increased by PDK2 knockdown or DCA treatment in SOD1G93A astrocytes. These results indicate that SOD1G93A astrocytes either have fewer mitochondria or their mitochondria undergo reduced respiratory activity, showing decreased ability to respond to energy demands. Significantly, this was reverted by the specific PDK2 siRNA treatment. These results indicate that the PDK2 isoform is a major determinant of astrocytic PDH activity state, as previously shown (Rahman et al., 2020).

Besides increasing mitochondrial respiratory function, the knockdown of PDK2 mRNA expression in SOD1G93A-bearing astrocytes modified their mitochondrial network morphology. During glial reactivity in ALS, astrocytes undergo a metabolic shift from OXPHOS to glycolysis, associated with mitochondrial morphology changes to adapt to the new metabolic system (Cassina et al., 2021). Mitochondria switches from a branched connected respiratory active elongated network into clustered, fragmented organelles with decreased OXPHOS, which has been previously described in several cell types (Galloway et al., 2012; Sauvanet et al., 2010) including SOD1G93A aberrant glial cells (Martínez-Palma et al., 2019). The significant decrease in mean mitochondrial length and the mean mitochondrial rod/branched length displayed by SOD1G93A astrocytes compared with non-Tg ones, along with fewer mitochondrial networks, indicates a higher organelle fragmentation in SOD1G93A astrocytes. PDK-silencing or DCA treatment induced a significant increase in the mentioned parameters, suggesting that mitochondria have coalesced into a complex network structure when increasing OXPHOS. Taken together, the detailed morphologic description and the respirometry data provide a complete overview of astrocyte mitochondria that may assist in identifying the subtle differences between healthy control and disease-associated SOD1G93A astrocytes.

The metabolic switch induced by PDK2 silencing reduced LDs content in SOD1G93A astrocytes. LDs are dynamic organelles that are regulated in response to different cellular and physiological conditions, including mitochondrial dysfunction (Renne & Hariri, 2021). The mitochondrial respiratory activity provides ATP and NADPH to support the synthesis of fatty acids and glycolytic precursors from the tricarboxylic acid cycle (e.g., citrate) for esterification into triacylglycerides in the endoplasmic reticulum and for the storage in LDs (Smolič, Zorec, & Vardjan, 2021). LDs increase in astrocytes submitted to hypoxia (Smolič et al., 2021) or ROS toxicity (Islam et al., 2019). Interestingly, SOD1G93A astrocytes have been shown to increase ROS formation (Vargas et al., 2006), and SOD1G93A aberrant glial cells exhibit a high amount of LDs by transmission electron microscopy (TEM) (Jiménez-Riani et al., 2017). Lipidomic analysis in the spinal cords of SOD1G93A rats showed an accumulation of lipids, mainly cholesteryl esters and ceramides, with further alterations linked to disease progression and a reduction in cardiolipin levels, reflecting mitochondrial adaptations (Chaves-Filho et al., 2019). The sequestration of lipids in droplets could reflect a protective mechanism against oxidative stress and lipotoxicity, avoiding lipid membrane peroxidation (Bailey et al., 2015; Olzmann & Carvalho, 2019). Our observation of LD reduction associated with an increase in mitochondrial OXPHOS activity further supports that a metabolic switch is occurring in SOD1G93A astrocytes after treatment.

A major finding of our work is that silencing PDK2 in SOD1G93A astrocytes restored their ability to support MN survival to the same extent achieved previously with mitochondrial-targeted strategies such as DCA or MitoQ (Cassina et al., 2021). The exact mechanism by which PDK2 inhibition is protecting MN survival needs further research. The link between mitochondrial OXPHOS and astrocyte-dependent trophic activity to MNs has been previously demonstrated with DCA (Martínez-Palma et al., 2019; Miquel et al., 2012), antioxidants, and nitric oxide synthase inhibitors (Cassina et al., 2008). As mitochondrial OXPHOS activity is a main source of reactive oxygen and nitrogen species (RONS) production, RONS-mediated signaling pathways may be involved in the trophic activity of astrocytes. In this

sense, the antioxidant response mediated by the nuclear factor erythroid 2-related factor 2 (Nrf2) has been shown to maintain the capacity of astrocytes to support MN survival (Díaz-Amarilla et al., 2016; Vargas et al., 2006). Taken together, these studies suggest that "mitochondrial dysfunction" in SOD1G93A astrocytes is not due to irreversible damage to the organelles but rather a metabolic adaptation to the neurodegenerative microenvironment. DCA is a PDK inhibitor (Stacpoole, 2017) with the same inhibitory action between different enzyme isoforms. Higher expression of PDK2 and PDK4 is revealed in astrocytes compared with neurons (Halim et al., 2010), which is consistent with the higher PDH $\alpha$  phosphorylation status, lower PDC activity, and higher lactate production displayed by cultured astrocytes (Pellerin & Magistretti, 2012). Then, PDK2 arises as a key target to modulate astrocytic mitochondrial function, reducing surrounding MN loss and inducing a diseasemodifying effect in ALS.

Previous transcriptomic analysis of glial and neuron from mice expressing enhanced green fluorescent protein (EGFP) under the control of cell-specific regulatory genes reported higher expression of PDK4 mRNA in astrocytes compared with neurons (Zhang et al., 2014, 2016). However, in astrocytes, higher expression levels of PDK2 compared with PDK4 have been reported in ALS mice (Guttenplan et al., 2020). In addition, the fact that PDK2 siRNA had no effect on PDK4 mRNA expression in astrocytes provides additional support for the choice of PDK2 as a target for regulating metabolic status in astrocytes.

Our results emphasize that mitochondrial function in astrocytes is a critical feature in maintaining the survival of neighboring MNs and indicate that inducing a cell-specific metabolic switch may offer a new therapeutic window to modulate astrocyte-mediated toxicity in ALS.

#### **AUTHOR CONTRIBUTIONS**

EM and PC conceived and planned the experiments. EM and RV performed the experiments. EM, RV, LMP, AC and PC analyzed the data and interpreted the results. EM and PC wrote and edited the manuscript. All the authors participated in the critical revision of the manuscript, added important intellectual content, and approved the definitive version.

#### **ACKNOWLEDGMENTS**

This work was supported by Grant # FCE\_1\_2019\_1\_156461 from the Agencia Nacional de Innovación e Investigación (ANII), Uruguay, to PC and Programa de Desarrollo de las Ciencias Básicas (PEDECIBA, MEC-UdelaR to PC and EM). We thank Dr. Homero Rubbo (Facultad de Medicina, Universidad de la República, Uruguay) for critical comments on the manuscript.

#### **CONFLICT OF INTEREST STATEMENT**

The authors declare no conflicts of interest.

#### **DATA AVAILABILITY STATEMENT**

The data that support the findings of this study are available from the corresponding author upon reasonable request.

#### ORCID

Ernesto Miquel https://orcid.org/0000-0002-4407-3661

Laura Martínez-Palma https://orcid.org/0000-0002-1094-5409

Patricia Cassina https://orcid.org/0000-0001-6606-489X

#### **REFERENCES**

- Al-Chalabi, A., Hardiman, O., Kiernan, M. C., Chiò, A., Rix-Brooks, B., & van den Berg, L. H. (2016). Amyotrophic lateral sclerosis: Moving towards a new classification system. *The Lancet Neurology*, 15, 1182–1194. https://doi.org/10.1016/S1474-4422(16)30199-5
- Bailey, A. P., Koster, G., Guillermier, C., Hirst, E. M. A., MacRae, J. I., Lechene, C. P., Postle, A. D., & Gould, A. P. (2015). Antioxidant role for lipid droplets in a stem cell niche of drosophila. *Cell*, 163(2), 340–353. https://doi.org/10.1016/j.cell.2015.09.020
- Bakare, A. B., Meshrkey, F., Lowe, B., Molder, C., Rao, R. R., Zhan, J., & Iyer, S. (2021). MitoCellPhe reveals mitochondrial morphologies in single fibroblasts and clustered stem cells. American Journal of Physiology—Cell Physiology, 321(4), C735–C748. https://doi.org/10.1152/ajpcell.00231.2021
- Bowker-Kinley, M. M., Davis, W. I., Wu, P., Harris, R. A., & Popov, K. M. (1998). Evidence for existence of tissue-specific regulation of the mammalian pyruvate dehydrogenase complex. *Biochemical Journal*, 329(1), 191–196. https://doi.org/10.1042/bj3290191
- Brand, M. D., & Nicholls, D. G. (2011). Assessing mitochondrial dysfunction in cells. *Biochemical Journal*, 435(2), 297–312. https://doi.org/10.1042/BJ20110162
- Cassina, P., Cassina, A., Pehar, M., Castellanos, R., Gandelman, M., de Leon, A., Robinson, K. M., Mason, R. P., Beckman, J. S., Barbeito, L., & Radi, R. (2008). Mitochondrial dysfunction in SOD1G93A-bearing astrocytes promotes motor neuron degeneration: Prevention by mitochondrial-targeted antioxidants. *Journal of Neuroscience*, 28(16), 4115–4122. https://doi.org/10.1523/JNEUROS CI.5308-07.2008
- Cassina, P., Miquel, E., Martínez-Palma, L., & Cassina, A. (2021). Glial metabolic reprogramming in amyotrophic lateral sclerosis. *Neuroimmunomo-dulation*, 28(4), 204–212. https://doi.org/10.1159/000516926
- Cassina, P., Peluffo, H., Pehar, M., Martínez-Palma, L., Ressia, A., Beckman, J. S., Estévez, A. G., & Barbeito, L. (2002). Peroxynitrite triggers a phenotypic transformation in spinal cord astrocytes that induces motor neuron apoptosis. *Journal of Neuroscience Research*, 67(1), 21–29. https://doi.org/10.1002/jnr.10107
- Chaves-Filho, A. B., Pinto, I. F. D., Dantas, L. S., Xavier, A. M., Inague, A., Faria, R. L., Medeiros, M. H. G., Glezer, I., Yoshinaga, M. Y., Miyamoto, S., & Miyamoto, S. (2019). Alterations in lipid metabolism of spinal cord linked to amyotrophic lateral sclerosis. *Scientific Reports*, 9(1), 11642. https://doi.org/10.1038/s41598-019-48059-7
- Clement, A. M., Nguyen, M. D., Roberts, E. A., Garcia, M. L., Boillée, S., Rule, M., McMahon, A. P., Doucette, W., Siwek, D., Ferrante, R. J., Brown, R. H., Jr., Julien, J.-P., Goldstein, L. S. B., & Cleveland, D. W. (2003). Wild-type nonneuronal cells extend survival of SOD1 mutant motor neurons in ALS mice. *Science*, 302(5642), 113–117. https://doi.org/10.1126/science.1086071
- Del Signore, S. J., Amante, D. J., Kim, J., Stack, E. C., Goodrich, S., Cormier, K., Smith, K., Cudkowicz, M. E., & Ferrante, R. J. (2009). Combined riluzole and sodium phenylbutyrate therapy in transgenic amyotrophic lateral sclerosis mice. *Amyotrophic Lateral Sclerosis*, 10(2), 85-94. https://doi.org/10.1080/17482960802226148
- Di Giorgio, F. P., Carrasco, M. A., Siao, M. C., Maniatis, T., & Eggan, K. (2007). Non-cell autonomous effect of glia on motor neurons in an embryonic stem cell-based ALS model. *Nature Neuroscience*, 10(5), 608-614. https://doi.org/10.1038/nn1885
- Díaz-Amarilla, P., Miquel, E., Trostchansky, A., Trias, E., Ferreira, A. M., Freeman, B. A., Cassina, P., Barbeito, L., Vargas, M. R., & Rubbo, H. (2016). Electrophilic nitro-fatty acids prevent astrocyte-mediated toxicity to motor neurons in a cell model of familial amyotrophic lateral

- sclerosis via nuclear factor erythroid 2-related factor activation. *Free Radical Biology and Medicine*, 95, 112–120. https://doi.org/10.1016/j.freeradbiomed.2016.03.013
- Díaz-Amarilla, P., Olivera-Bravo, S., Trias, E., Cragnolini, A., Martínez-Palma, L., Cassina, P., Beckman, J., & Barbeito, L. (2011). Phenotypically aberrant astrocytes that promote motoneuron damage in a model of inherited amyotrophic lateral sclerosis. *Proceedings of the National Academy of Sciences*, 108(44), 18126–18131. https://doi.org/10.1073/pnas.1110689108
- Fan, J., Kang, H.-B., Shan, C., Elf, S., Lin, R., Xie, J., Gu, T.-L., Aguiar, M., Lonning, S., Chung, T.-W., Arellano, M., Khoury, H. J., Shin, D. M., Khuri, F. R., Boggon, T. J., Kang, S., & Chen, J. (2014). Tyr-301 phosphorylation inhibits pyruvate dehydrogenase by blocking substrate binding and promotes the Warburg effect. *Journal of Biological Chemistry*, 289(38), 26533–26541. https://doi.org/10.1074/jbc.M114.593970
- Ferriero, R., Iannuzzi, C., Manco, G., & Brunetti-Pierri, N. (2015). Differential inhibition of PDKs by phenylbutyrate and enhancement of pyruvate dehydrogenase complex activity by combination with dichloroacetate. *Journal of Inherited Metabolic Disease*, 38(5), 895–904. https://doi.org/10.1007/s10545-014-9808-2
- Galloway, C. A., Lee, H., & Yoon, Y. (2012). Mitochondrial morphology— Emerging role in bioenergetics. Free Radical Biology and Medicine, 53(12), 2218–2228. https://doi.org/10.1016/j.freeradbiomed.2012. 09.035
- Guttenplan, K. A., Weigel, M. K., Adler, D. I., Couthouis, J., Liddelow, S. A., Gitler, A. D., & Barres, B. A. (2020). Knockout of reactive astrocyte activating factors slows disease progression in an ALS mouse model. *Nature Communications*, 11(1), 1–9. https://doi.org/10.1038/s41467-020-17514-9
- Haidet-Phillips, A. M., Hester, M. E., Miranda, C. J., Meyer, K., Braun, L., Frakes, A., Song, S. W., Likhite, S., Murtha, M. J., Foust, K. D., Rao, M., Eagle, A., Kammesheidt, A., Christensen, A., Mendell, J. R., Burghes, A. H. M., & Kaspar, B. K. (2011). Astrocytes from familial and sporadic ALS patients are toxic to motor neurons. *Nature Biotechnology*, 29(9), 824–828. https://doi.org/10.1038/nbt.1957
- Halim, N. D., Mcfate, T., Mohyeldin, A., Okagaki, P., Korotchkina, L. G., Patel, M. S., & Verma, A. (2010). Phosphorylation status of pyruvate dehydrogenase distinguishes metabolic phenotypes of cultured rat brain astrocytes and neurons. *Glia*, 58(10), 1168–1176. https://doi. org/10.1002/glia.20996
- Hasel, P., Rose, I. V. L., Sadick, J. S., Kim, R. D., & Liddelow, S. A. (2021). Neuroinflammatory astrocyte subtypes in the mouse brain. *Nature Neuroscience*, 24(10), 1475–1487. https://doi.org/10.1038/s41593-021-00905-6
- Hiromasa, Y., Fujisawa, T., Aso, Y., & Roche, T. E. (2004). Organization of the cores of the mammalian pyruvate dehydrogenase complex formed by E2 and E2 plus the E3-binding protein and their capacities to bind the E1 and E3 components. *Journal of Biological Chemistry*, 279(8), 6921–6933. https://doi.org/10.1074/jbc.M308172200
- Hitosugi, T., Fan, J., Chung, T.-W., Lythgoe, K., Wang, X., Xie, J., Ge, Q., Gu, T.-L., Polakiewicz, R. D., Roesel, J. L., Chen, G. Z., Boggon, T. J., Lonial, S., Fu, H., Khuri, F. R., Kang, S., & Chen, J. (2011). Tyrosine phosphorylation of mitochondrial pyruvate dehydrogenase kinase 1 is important for cancer metabolism. *Molecular Cell*, 44(6), 864–877. https://doi.org/10.1016/j.molcel.2011.10.015
- Holness, M. J., Bulmer, K., Smith, N. D., & Sugden, M. C. (2003). Investigation of potential mechanisms regulating protein expression of hepatic pyruvate dehydrogenase kinase isoforms 2 and 4 by fatty acids and thyroid hormone. *Biochemical Journal*, 369(3), 687–695. https://doi.org/10.1042/bj20021509
- Howland, D. S., Liu, J., She, Y., Goad, B., Maragakis, N. J., Kim, B., Erickson, J., Kulik, J., DeVito, L., Psaltis, G., DeGennaro, L. J., Cleveland, D. W., & Rothstein, J. D. (2002). Focal loss of the glutamate transporter EAAT2 in a transgenic rat model of SOD1 mutant-mediated amyotrophic lateral sclerosis (ALS). Proceedings of the

- National Academy of Sciences, 99(3), 1604–1609. https://doi.org/10.1073/pnas.032539299
- Islam, A., Kagawa, Y., Miyazaki, H., Shil, S. K., Umaru, B. A., Yasumoto, Y., Yamamoto, Y., & Owada, Y. (2019). FABP7 protects astrocytes against ROS toxicity via lipid droplet formation. *Molecular Neurobiology*, 56(8), 5763–5779. https://doi.org/10.1007/s12035-019-1489-2
- Jha, M. K., Jeon, S., & Suk, K. (2012). Pyruvate dehydrogenase kinases in the nervous system: Their principal functions in neuronal-glial metabolic interaction and neuro-metabolic disorders. Current Neuropharmacology, 10(4), 393–403. https://doi.org/10.2174/1570159128044 99528
- Jiménez-Riani, M., Díaz-Amarilla, P., Isasi, E., Casanova, G., Barbeito, L., & Olivera-Bravo, S. (2017). Ultrastructural features of aberrant glial cells isolated from the spinal cord of paralytic rats expressing the amyotrophic lateral sclerosis-linked SOD1G93A mutation. Cell and Tissue Research, 370(3), 391–401. https://doi.org/10.1007/s00441-017-2681-1
- Joshi, A. U., Minhas, P. S., Liddelow, S. A., Haileselassie, B., Andreasson, K. I., Dorn, G. W., & Mochly-Rosen, D. (2019). Fragmented mitochondria released from microglia trigger A1 astrocytic response and propagate inflammatory neurodegeneration. *Nature Neu*roscience, 22(10), 1635–1648. https://doi.org/10.1038/s41593-019-0486-0
- Kolobova, E., Tuganova, A., Boulatnivov, I., & Popov, K. M. (2001). Regulation of pyruvate dehydrogenase activity through phosphorylation at multiple sites. *Biochemical Journal*, 358(1), 69–77. https://doi.org/10.1042/0264-6021:3580069
- Leonard, A. P., Cameron, R. B., Speiser, J. L., Wolf, B. J., Peterson, Y. K., Schnellmann, R. G., Beeson, C. C., & Rohrer, B. (2015). Quantitative analysis of mitochondrial morphology and membrane potential in living cells using high-content imaging, machine learning, and morphological binning. *Biochimica et Biophysica Acta*, 1853(2), 348–360. https://doi.org/10.1016/j.bbamcr.2014.11.002
- Liu, L., Zhang, K., Sandoval, H., Yamamoto, S., Jaiswal, M., Sanz, E., Li, Z., Hui, J., Graham, B. H., Quintana, A., & Bellen, H. J. (2015). Glial lipid droplets and ROS induced by mitochondrial defects promote neurodegeneration. *Cell*, 160(1-2), 177-190. https://doi.org/10.1016/j.cell. 2014.12.019
- Lydell, C. P., Chan, A., Wambolt, R. B., Sambandam, N., Parsons, H., Bondy, G. P., Rodrigues, B., Popov, K. M., Harris, R. A., Brownsey, R. W., & Allard, M. F. (2002). Pyruvate dehydrogenase and the regulation of glucose oxidation in hypertrophied rat hearts. *Cardio-vascular Research*, 53(4), 841–851. https://doi.org/10.1016/s0008-6363(01)00560-0
- Martínez-Palma, L., Miquel, E., Lagos-Rodríguez, V., Barbeito, L., Cassina, A., & Cassina, P. (2019). Mitochondrial modulation by dichloroacetate reduces toxicity of aberrant glial cells and gliosis in the SOD1G93A rat model of amyotrophic lateral sclerosis. Neurotherapeutics, 16(1), 203–215. https://doi.org/10.1007/s13311-018-0659-7
- Miquel, E., Cassina, A., Martínez-Palma, L., Bolatto, C., Trías, E., Gandelman, M., Radi, R., Barbeito, L., & Cassina, P. (2012). Modulation of astrocytic mitochondrial function by dichloroacetate improves survival and motor performance in inherited amyotrophic lateral sclerosis. PLoS One, 7(4), e34776. https://doi.org/10.1371/journal.pone. 0034776
- Nagai, M., Re, D. B., Nagata, T., Chalazonitis, A., Jessell, T. M., Wichterle, H., & Przedborski, S. (2007). Astrocytes expressing ALSlinked mutated SOD1 release factors selectively toxic to motor neurons. *Nature Neuroscience*, 10(5), 615–622. https://doi.org/10.1038/ nn1876
- Olzmann, J. A., & Carvalho, P. (2019). Dynamics and functions of lipid droplets. *Nature Reviews Molecular Cell Biology*, 20(3), 137–155. https://doi.org/10.1038/s41580-018-0085-z
- Paganoni, S., Macklin, E. A., Hendrix, S., Berry, J. D., Elliott, M. A., Maiser, S., Karam, C., Caress, J. B., Owegi, M. A., Quick, A., Wymer, J.,

- Goutman, S. A., Heitzman, D., Heiman-Patterson, T., Jackson, C. E., Quinn, C., Rothstein, J. D., Kasarskis, E. J., Katz, J., ... Cudkowicz, M. E. (2020). Trial of sodium phenylbutyrate-taurursodiol for amyotrophic lateral sclerosis. *New England Journal of Medicine*, 383(10), 919–930. https://doi.org/10.1056/NEJMoa1916945
- Palamiuc, L., Schlagowski, A., Ngo, S. T., Vernay, A., Dirrig-Grosch, S., Henriques, A., Boutillier, A.-L., Zoll, J., Echaniz-Laguna, A., Loeffler, J.-P., & René, F. (2015). A metabolic switch toward lipid use in glycolytic muscle is an early pathologic event in a mouse model of amyotrophic lateral sclerosis. EMBO Molecular Medicine, 7(5), 526– 546. https://doi.org/10.15252/emmm.201404433
- Patel, M. S., & Korotchkina, L. G. (2006). Regulation of the pyruvate dehydrogenase complex. *Biochemical Society Transactions*, 34(2), 217. https://doi.org/10.1042/BST20060217
- Patel, M. S., & Roche, T. E. (1990). Molecular biology and biochemistry of pyruvate dehydrogenase complexes 1. The FASEB Journal, 4(14), 3224–3233. https://doi.org/10.1096/fasebj.4.14.2227213
- Pellerin, L., & Magistretti, P. J. (2012). Sweet sixteen for ANLS. Journal of Cerebral Blood Flow & Metabolism, 32(7), 1152–1166. https://doi.org/ 10.1038/jcbfm.2011.149
- Pharaoh, G., Sataranatarajan, K., Street, K., Hill, S., Gregston, J., Ahn, B., Kinter, C., Kinter, M., & Van Remmen, H. (2019). Metabolic and stress response changes precede disease onset in the spinal cord of mutant SOD1 ALS mice. Frontiers in Neuroscience, 13, 487. https://doi.org/10.3389/fnins.2019.00487
- Rahman, M. H., Bhusal, A., Kim, J.-H., Jha, M. K., Song, G. J., Go, Y., Jang, I.-S., Lee, I.-K., & Suk, K. (2020). Astrocytic pyruvate dehydrogenase kinase-2 is involved in hypothalamic inflammation in mouse models of diabetes. *Nature Communications*, 11(1), 5906. https://doi.org/10.1038/s41467-020-19576-1
- Renne, M. F., & Hariri, H. (2021). Lipid droplet-organelle contact sites as hubs for fatty acid metabolism, trafficking, and metabolic channeling. Frontiers in Cell and Developmental Biology, 14(9), 726261. https://doi. org/10.3389/fcell.2021.726261
- Ryu, H., Smith, K., Camelo, S. I., Carreras, I., Lee, J., Iglesias, A. H., Dangond, F., Cormier, K. A., Cudkowicz, M. E., Brown, R. H., Jr., & Ferrante, R. J. (2005). Sodium phenylbutyrate prolongs survival and regulates expression of anti-apoptotic genes in transgenic amyotrophic lateral sclerosis mice. *Journal of Neurochemistry*, 93(5), 1087–1098. https://doi.org/10.1111/j.1471-4159.2005.03077.x
- Saneto, R., & De Vellis, J. (1987). Neuronal and glial cells: Cell culture of the central nervous system. In A. Turner & H. Brachelard (Eds.), Neurochemistry: A practical approach (pp. 27–63). Oxford IRL Press.
- Sauvanet, C., Duvezin-Caubet, S., di Rago, J.-P., & Rojo, M. (2010). Energetic requirements and bioenergetic modulation of mitochondrial morphology and dynamics. Seminars in Cell & Developmental Biology, 21(6), 558–565. https://doi.org/10.1016/j.semcdb.2009.12.006
- Smith, E. F., Shaw, P. J., & De Vos, K. J. (2019). The role of mitochondria in amyotrophic lateral sclerosis. *Neuroscience Letters*, 710, 132933. https://doi.org/10.1016/j.neulet.2017.06.052
- Smolič, T., Tavčar, P., Horvat, A., Černe, U., Halužan Vasle, A., Tratnjek, L., Kreft, M. E., Scholz, N., Matis, M., Petan, T., Zorec, R., & Vardjan, N. (2021). Astrocytes in stress accumulate lipid droplets. *Glia*, 69(6), 1540–1562. https://doi.org/10.1002/glia.23978
- Smolič, T., Zorec, R., & Vardjan, N. (2021). Pathophysiology of lipid droplets in neuroglia. Antioxidants, 11(1), 22. https://doi.org/10.3390/ antiox11010022
- Stacpoole, P. W. (2017). Therapeutic targeting of the pyruvate dehydrogenase complex/pyruvate dehydrogenase kinase (PDC/PDK) axis in cancer. *JNCI: Journal of the National Cancer Institute*, 109(11), 1–14. https://doi.org/10.1093/jnci/djx071
- Takubo, K., Nagamatsu, G., Kobayashi, C. I., Nakamura-Ishizu, A., Kobayashi, H., Ikeda, E., Goda, N., Rahimi, Y., Johnson, R. S., Soga, T., Hirao, A., Suematsu, M., & Suda, T. (2013). Regulation of glycolysis by Pdk functions as a metabolic checkpoint for cell cycle quiescence in

- hematopoietic stem cells. *Cell Stem Cell*, 12(1), 49-61. https://doi.org/10.1016/j.stem.2012.10.011
- Taylor, J. P., Brown, R. H., & Cleveland, D. W. (2016). Decoding ALS: From genes to mechanism. *Nature*, 539(7628), 197–206. https://doi.org/10.1038/nature20413
- Valente, A. J., Maddalena, L. A., Robb, E. L., Moradi, F., & Stuart, J. A. (2017). A simple ImageJ macro tool for analyzing mitochondrial network morphology in mammalian cell culture. *Acta Histochemica*, 119(3), 315–326. https://doi.org/10.1016/j.acthis.2017.03.001
- Vargas, M. R., Pehar, M., Cassina, P., Beckman, J. S., & Barbeito, L. (2006). Increased glutathione biosynthesis by Nrf2 activation in astrocytes prevents p75NTR-dependent motor neuron apoptosis. *Journal of Neu*rochemistry, 97(3), 687-696. https://doi.org/10.1111/j.1471-4159. 2006.03742.x
- Velebit, J., Horvat, A., Smolič, T., Prpar Mihevc, S., Rogelj, B., Zorec, R., & Vardjan, N. (2020). Astrocytes with TDP-43 inclusions exhibit reduced noradrenergic cAMP and Ca2+ signaling and dysregulated cell metabolism. *Scientific Reports*, 10(1), 6003. https://doi.org/10.1038/s41598-020-62844-5
- Zhang, W., Zhang, S.-L., Hu, X., & Tam, K. Y. (2015). Targeting tumor metabolism for cancer treatment: Is pyruvate dehydrogenase kinases (PDKs) a viable anticancer target? *International Journal of Biological Sciences*, 11(12), 1390–1400. https://doi.org/10.7150/ijbs.13325
- Zhang, Y., Chen, K., Sloan, S. A., Bennett, M. L., Scholze, A. R., Keeffe, S. O., Phatnani, H. P., Guarnieri, P., Caneda, C., Ruderisch, N.,

- Deng, S., Liddelow, S. A., Zhang, C., Daneman, R., Maniatis, T., Barres, B. A., & Wu, X. J. Q. (2014). An RNA-sequencing transcriptome and splicing database of glia, neurons, and vascular cells of the cerebral cortex. *Journal of Neuroscience*, *34*(36), 11929–11947. https://doi.org/10.1523/JNEUROSCI.1860-14.2014
- Zhang, Y., Sloan, S. A., Clarke, L. E., Caneda, C., Plaza, C. A., Blumenthal, P. D., Vogel, H., Steinberg, G. K., Edwards, M. S. B., Li, G., Duncan, J. A., 3rd, Cheshier, S. H., Shuer, L. M., Chang, E. F., Grant, G. A., Hayden Gephart, M. G., & Barres, B. A. (2016). Purification and characterization of progenitor and mature human astrocytes reveals transcriptional and functional differences with mouse. *Neuron*, 89(1), 37–53. https://doi.org/10.1016/J.NEURON.2015.11.013

How to cite this article: Miquel, E., Villarino, R., Martínez-Palma, L., Cassina, A., & Cassina, P. (2024). Pyruvate dehydrogenase kinase 2 knockdown restores the ability of amyotrophic lateral sclerosis-linked SOD1G93A rat astrocytes to support motor neuron survival by increasing mitochondrial respiration. *Glia*, 72(5), 999–1011. <a href="https://doi.org/10.1002/glia.24516">https://doi.org/10.1002/glia.24516</a>